*IJST (2014) 38A4: 389-397*
***Iranian Journal of Science & Technology***

http://ijsts.shirazu.ac.ir

# Numerical solution of Reynold's equation governing noncircular gas bearing system using radial basis function

H. Rasooli Shooroki[1]*, R. Rashidi Meybodi[2], S. M. Karbassi[3] and G. B. Loghmani[1]

[1]*Faculty of Mathematics, Yazd University, Yazd, Iran*
[2]*Department of Mechanical Engineering, Payame Noor University, Tehran, Iran*
[3]*Faculty of Advanced Education, Islamic Azad University, Yazd Branch, Yazd, Iran*
*E-mail: rasoolishoroky@gmail.com*

## Abstract

In this paper, the static characteristics of two-lobe, three-lobe and four-lobe noncircular gas journal bearing systems are studied in detail. The Reynold's equation governing the noncircular gas bearing systems are analyzed by using Radial Basis Functions (RBF). The solutions are obtained numerically by solving systems of algebraic equations. The equilibrium position of the rotor is obtained without using the trial and error method; which is the merit of our method.

***Keywords****:* Reynold's equation; noncircular gas bearings; radial basis function

## 1. Introduction

Many problems in physics and engineering are reduced to a set of differential equations in a mathematical model. It is not always easy to obtain their exact solution, so numerical methods are a useful option to use instead.

In the last decade, the numerical solution of the various types of partial differential equations (PDEs) has been obtained by meshless methods. The development of the meshless method is required to alleviate the meshing problems associated with methods such as the finite element and finite difference (Dag and Dereli, 2008). Various meshless methods have been developed. Meshless methods based on the collocation method have been dominant and very efficient (Dag and Dereli, 2008).

For the last 20 years, the radial basis functions method has been known as a powerful tool for the scattered data interpolation problem. The use of radial basis functions as a meshless procedure for numerical solution of partial differential equationsis based on the collocation scheme. Due to the collocation technique, this method does not need to evaluate any integral. The main advantage of numerical procedures, which use radial basis functions over traditional techniques, is the meshless property of these methods (Dehghan and Shokri, 2009). Radial basis functions are used actively for solving partial differential equations (Kansa, 1990; Zerroukat et al., 1998; Chen et al., 2012; Islam et al., 2012).

The journal bearings have been widely used in rotating machinery. Reynold's equations are the base for bearing static and dynamic analysis. The governing equations are a set of PDEs. The equation considered in this paper is a nonlinear PDE, which is very difficult to solve analytically. The commonly used numerical methods for solving Reynold's equations include finite difference method (FDM) (Lund and Thomsen, 1978) and finite element method (FEM) (Klit and Lund, 1986). Wang et al. (2007) investigated dynamic behavior of gas bearings system by using FDM. FEM is also used for solving Reynold's equation. Reddi (1969) used FEM for incompressible lubricant and Reddi et al. (1970) used the FEM for compressible lubricant. Then this method was used in lubrication with compressible fluid for different problems. Rahmatabadi and Rashidi (2007) used it for investigation of static and dynamic characteristics in noncircular gas bearings system. The nonlinear dynamic behavior in such systems by using the parameters such as rotor mass, bearing number and preload has been investigated (Rashidi et al., 2010). FEM is the concept of finding approximate solutions to PDEs, which are broken up into a number of elements. It is usually assumed that the approximate solutions vary linearly over

*Corresponding author
Received: 30 January 2013 / Accepted: 1 June 2014

each individual element. This fact may be true only for the case of sufficiently small elements. An efficient method for solving Reynold's equation is still being investigated (Jiangang et al., 2008). Gustavo et al. (2011) proposed an analytical approximate solution of the Reynold's equation for isothermal finite length journal bearings by means of the regular perturbation method. They obtained a solution by which they could give an analytical tool for the description of pressure. Kansa's RBF method has been used for solving Reynold's equation governing circular journal bearings for finding characteristics of the system by Jiangagng et.al (2008). In this paper, we focus our attention on solving Reynold's equation using RBFs to calculate the equilibrium point of rotor, which is important for investigating behavior of system in dynamical state. The aim is to overcome the problems in the previous methods. The equilibrium point in previous method (Rahmatabadi and Rashidi, 2007; Chandra and Sinhasan, 1983) was obtained by trial and error test but in this work the equilibrium point is obtained directly and pressure distribution is displayed as a continuous function for three types; two, three and four lobe noncircular journal bearings (See Fig. 1).

The layout of the rest of this paper is as follows: In Section 2 we introduce radial basis functions to approximate the solution. In Section 3 we give a brief introduction to Reynold's equation governing noncircular gas journal bearings. In Section 4 the numerical method is explained. Section 5 is dedicated to results and discussion. An error analysis for the proposed method is introduced in Section 6. Finally, Section 7 is dedicated to a brief conclusion.

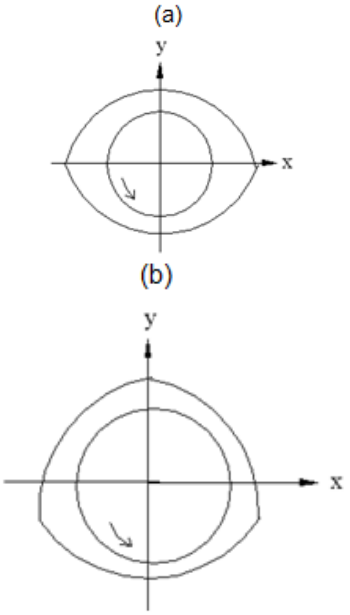


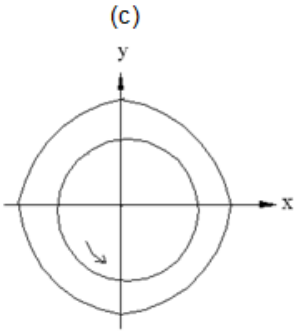


**Fig. 1.** Noncircular journal bearing configurations: (a) two lobe, (b) three lobe and (c) four lobe

## 2. Radial basis functions

Here we briefly recall the theory behind radial basis functions also known as RBFs.

### *2.1 Definition of radial basis function*

Let $R^+ = \{x \in R, x \geq 0\}$ and let $\phi: R^+ \to R$ be a continuous function with $\phi(0) \geq 0$. A radial basis function (RBF) on $R^d$ is a function of the form $\phi(\| X - X_i \|)$, where $X, X_i \in R^d$ and $\|.\|$ denotes the Euclidean distance between X and $X_i$'s. If one chooses N points $\{X_i\}_{i=1}^N$ in $R^d$ then

$$s(X) = \sum_{i=1}^{N} \lambda_i \, \phi(\| X - X_i \|), \quad \lambda_i \in R, \tag{1}$$

is called a radial basis function as well (Parand and Rad, 2012; Baxter, 1992; Golberg, 1999). The standard radial basis functions are categorized into two major classes, infinitely smooth and piecewise smooth. Infinitely smooth functions are infinitely differentiable and depend heavily on the shape parameter c, see Table 1. Piecewise smooth functions are not infinitely differentiable and are shape parameter free, see Table 2.

**Table 1.** Some commonly used infinitely smooth RBF

| Infinitely smooth RBFs | $\phi(r)$ |
|---|---|
| Gussian(GA) | $e^{-c^2r^2}$ |
| Inverse multiquadric (IMQ) | $1/\sqrt{c^2 + r^2}$ |
| Inverse quadric(IQ) | $1/(c^2 + r^2)$ |
| Multiquadric (MQ) | $\sqrt{c^2 + r^2}$ |

**Table 2.** Some commonly used piecewise smooth RBFs

| Piecewise Smooth | $\phi(r)$ |
|---|---|
| Thin plate spline | $r^2 lnr$ |
| Generalized thin plate spline | $\begin{cases} r^{2k}\log r & k \in N \\ r^{2\upsilon} & \upsilon \notin N \end{cases}$ |
| Cubic spline | $r^3$ |
| Wendland functions | $(1-r)_+^k P(r), \ k \in N$ |

*2.2. Radial Basis function approximation*

The approximation of a function u(x), using radial basis functions, may be written as a linear combination of N radial functions; it usually takes the following form:

$$u(x) \simeq \sum_{j=}^{N} \lambda_j \phi(X, X_j) + \psi(X) \text{ for} X \epsilon \Omega \subset R^d, \quad (2)$$

where N is the number of data points, $X = (x_1, x_2, \dots, x_d)$, d is the dimension of the problem, $\lambda_i$'s are coefficients to be determined and $\phi$ is the radial basis function. Equation (2) can be written without the additional polynomial $\psi$. In that case, $\phi$ must be unconditionally positive definite to guarantee the solvability of the resulting system for example, Gaussian and multi-quadrics. Gaussian RBF will be used for the numerical scheme introduced in Section 4.

## 3. Mathematical Analysis

Here we briefly describe the governing equations and the mathematical analysis of the problem.

*3.1. Governing Equation*

Analysis of gas lubricated noncircular bearing, involves solution of the governing equations separately for an individual lobe of the bearing, treating each lobe as an independent partial bearing. To generalize the analysis for all noncircular geometries, the film geometry of each lobe is described with reference to bearing fixed Cartesian axes (Fig. 2). Thus the film thickness in the clearance space of the $k^{th}$ lobe, with the journal in a state of translatory whirl, is expressed in the steady state as (Chandra et al., 1983):

$${h_0}^k = \frac{1}{\delta} - x_{j_0} \cos\theta - y_{j_0} \sin\theta + \left(\frac{1}{\delta} - 1\right) \cos(\theta - {\theta_0}^k), \quad (3)$$

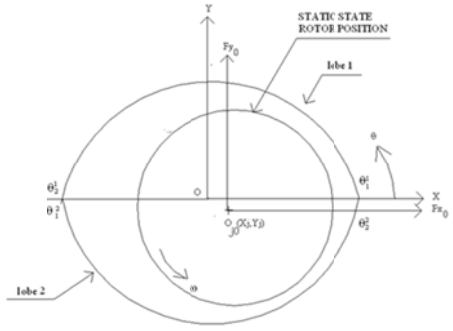


**Fig. 2.** Noncircular two-lobe bearing geometry and coordinate axes

$(x_{j_0}, y_{j_0})$ is the steady state journal center coordinates, $\delta$ is preload and $\theta_0^k$ is angle of lobe line of centers.

The pressure governing equation of isothermal flow field in a bearing lobe is [24]:

$$\frac{\partial}{\partial\theta}\left\{{h_0}^3(P_0+1)\frac{\partial P_0}{\partial\theta}\right\} + \frac{\partial}{\partial\xi}\left\{{h_0}^3(P_0+1)\frac{\partial P_0}{\partial\xi}\right\} = \Lambda\frac{\partial}{\partial\theta}\{(P_0+1)h_0\}, \quad (4)$$

Subjected to the conditions:

$$P_0(\theta, \lambda) = 0 \ , P_0(\theta, -\lambda) = 0, \quad (5)$$

$$P_0({\theta_1}^k, \xi) = 0, P_0({\theta_2}^k, \xi) = 0, \qquad k = 1, 2. \quad (6)$$

where $\theta_1^k$ and $\theta_2^k$ are the leading and trailing edge boundaries of $k^{th}$ lobe respectively, and

$$\Lambda = \frac{6\,\bar{\mu}\bar{\omega_0}\overline{R^2}}{\bar{P_a}\overline{C_m^2}}, \quad (7)$$

is the dimensionless parameter called the compressibility number or bearing number.
The Equation (4) is the nonlinear PDE. In this work, the solution of this equation is obtained by RBF collocation method.

*3.2. Static Characteristics*

Having obtained the steady state pressure field by the solution of Equation (4), the static characteristics are obtained. The static characteristics are described by the bearing load capacity, the attitude angle and the viscous power loss. The components of the gas film force on the journal are given by:

$$\begin{bmatrix} F_{x_0} \\ F_{y_0} \end{bmatrix} = \sum_{k=1}^{L} \begin{bmatrix} {F_{x_0}}^k \\ {F_{y_0}}^k \end{bmatrix} = -\sum_{k=1}^{L} \int_{-\lambda}^{\lambda} \int_{\theta_1^k}^{\theta_2^k} P_{0_k} \begin{bmatrix} \cos\theta \\ \sin\theta \end{bmatrix} d\theta d\xi, \quad (8)$$

where L stands for the number of lobes.

The load capacity and the attitude angle are then given by:

$$\begin{cases} F_0 = (F_{x_0}^2 + F_{y_0}^2)^{1/2} \\ \phi_0 = \arctan\left(\dfrac{X_{j_0}}{Y_{j_0}}\right), \end{cases} \quad (9)$$

and the viscous power loss is given by (Khattak et al., 2009):

$$P_{\mathrm{L}} = \sum_{k=1}^{L} \int_{-\lambda}^{\lambda} \int_{\theta_1^k}^{\theta_2^k} \left( \frac{3h_{0_k}}{\Lambda} \frac{\partial P_{0_k}}{\partial \theta} + \frac{1}{h_{0_k}} \right) d\theta \, d\xi, \qquad (10)$$

## 4. Numerical Method

In this study, we explain the method for two lobe bearing; this can be extended to the three lobe and four lobe bearings similarly. Here, the object is to find the coordinates of the equilibrium of the center point of the rotor. Then, calculation of energy loss is intended. To obtain the equilibrium of the center point, it is necessary to obtain the pressure function governing the system. The problem of two lobe is different for the function ${h_0}^k(\theta),\ k = 1,2$ based on ${\theta_0}^k, k = 1,2$ so that the form of the differential Equation (4) for each lobe is different. For this reason, since our object is to find the pressure function on the system and simultaneously to obtain the equilibrium point $(x, y)$, the function $P_0(\theta, \xi)$ is considered as follows:

$$P_0(\theta,\xi) = \begin{cases} {P_0}^{(1)}(\theta,\xi), & {\theta_1}^1 \le \theta \le {\theta_2}^1 \\ {P_0}^{(2)}(\theta,\xi), & {\theta_1}^2 \le \theta \le {\theta_2}^2 \end{cases}, \quad -\lambda < \xi < \lambda, \qquad (11)$$

Now for the function $\mathrm{P_0}(\theta,\xi)$ to be continuous at $\theta = {\theta_2}^1 = {\theta_1}^2 = \pi$, the boundary conditions Equations (5) and (6) for $\mathrm{P_0}^{\mathrm{k}}(\theta,\xi),\ \mathrm{k} = 1,2$ can be rewritten as:

$${P_0}^{(k)}\left({\theta_1}^k, \xi\right) = 0, {P_0}^{(k)}\left({\theta_2}^k, \xi\right) = 0, \qquad (12)$$

$${P_0}^{(k)}(\theta, \lambda) = 0, {P_0}^{(k)}(\theta, -\lambda) = 0\,, \qquad (13)$$

Now, consider an approximate solution to the analytic solution ${P_0}^{(1)}(\theta,\xi)$ and ${P_0}^{(2)}(\theta,\xi)$ in the radial basis function forms:

$${P_0}^{(1)}(\theta,\xi) = \sum_{i=0}^{\frac{N}{2}} \sum_{j=0}^{M} {\alpha^{(1)}}_{i,j} {\phi^1}_{i,j}(\theta,\xi), \qquad (14)$$

$${P_0}^{(2)}(\theta,\xi) = \sum_{i=\frac{N}{2}}^{N} \sum_{j=0}^{M} {\alpha^{(2)}}_{i,j} {\phi^2}_{i,j}(\theta,\xi), \qquad (15)$$

where $\alpha^{(\mathrm{k})}_{\mathrm{i,j}},\ \mathrm{k} = 1,2$ are the coefficients to be determined. Here N and M are the number of data points on axis θ and ξ, respectively. It should be noted that N must be taken as a multiple of the lobe under consideration. ${\phi^k}_{i,j}(\theta,\xi),\ k = 1,2$ is defined as:

$${\phi^1}_{i,j}(\theta,\xi) = \phi\left(\sqrt{(\theta - \widetilde{\theta_i^k})^2 + (\xi - \widetilde{\xi_j^k})^2}\right), \qquad (16)$$

$${\phi_{i,j}}^2(\theta,\xi) = \phi\left(\sqrt{(\theta - \widetilde{\theta_i^k})^2 + (\xi - \widetilde{\xi_j^k})^2}\right), \qquad (17)$$

Here ϕ is Gaussian radial basis functions and

$$\widetilde{\theta_i^1} = {\theta_1}^1 + i\frac{{\theta_2}^1 - {\theta_1}^1}{N}, i = 0,1,\ldots,\frac{N}{2}, \qquad (18)$$

$$\widetilde{\theta_i^2} = {\theta_1}^2 + i\frac{{\theta_2}^2 - {\theta_1}^2}{N}, i = \frac{N}{2}, \frac{N}{2} + 1, \ldots, N, \qquad (19)$$

$$\widetilde{\xi_j^k} = \lambda\left(\frac{2j}{M} - 1\right), j = 0,1,2,\ldots,M, \quad k = 1,2, \qquad (20)$$

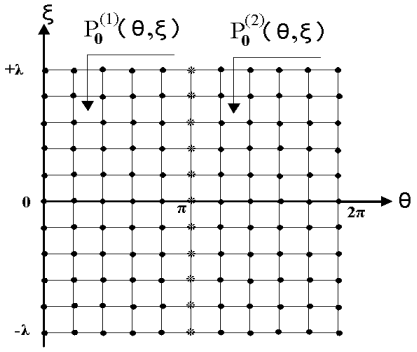


**Fig. 3.** The grid points of θ, ξ

By using (4)-(6) and (9) to calculate $\mathrm{P_0}(\theta,\xi)$, we need to compute $2\left(\frac{N}{2}+1\right)(M+1)+2$ unknown parameters $\alpha^{(1)}_{\mathrm{i,j}}, i = 0,1,2,\ldots,\frac{N}{2}, j = 0,1,2,\ldots,M$ and $\alpha^{(2)}_{i,j}$, $i = \frac{N}{2}, \frac{N}{2}+1, \frac{N}{2}+2, \ldots, N,\ j = 0,1,2,\ldots,M$ and $x, y$ Therefore, we require a set of $\mathrm{k}\left(\frac{\mathrm{N}}{2}+1\right)(\mathrm{M}+1)+2$ equations.
We define:

$$RES^k(\theta,\xi) = \frac{\partial}{\partial\theta}\left\{(h_0{}^k)^3\left({P_0}^{(k)}+1\right)\frac{\partial {P_0}^{(k)}}{\partial\theta}\right\} + \frac{\partial}{\partial\xi}\left\{(h_0{}^k)^3\left({P_0}^{(k)}+1\right)\frac{\partial {P_0}^{(k)}}{\partial\xi}\right\} - \Lambda\frac{\partial}{\partial\theta}\left\{\left({P_0}^{(k)}+1\right)h_0{}^k\right\},\ k = 1,2. \qquad (21)$$

Since $F_x = 0\,, F_y = W_0$, then as in [25] it follows that:

$$F_x = -\int_{-\lambda}^{\lambda}\int_{0}^{2\pi} P_0(\theta,\xi)\cos(\theta,\xi)d\theta d\xi, \qquad (22)$$

$$F_y = -\int_{-\lambda}^{\lambda}\int_{0}^{2\pi} P_0(\theta,\xi)\,sin(\theta,\xi)d\theta d\xi, \qquad (23)$$

Now, by using the collocation points (18)-(20) and considering Fig. 3 the following equations are obtained:

$$RES^1\left(\widetilde{\theta_i^1}, \widetilde{\xi_j^1}\right) = 0, \quad i = 1,\ldots,\tfrac{N}{2}-1\ ;\ j = 1,2,\ldots,M-1, \qquad (24)$$

$$RES^2\left(\widetilde{\theta_i^2}, \widetilde{\xi_j^2}\right) = 0, \quad i = \tfrac{N}{2}+1,\ldots,N-1\ ;\ j = 1,2,\ldots,\mathrm{M}-1. \qquad (25)$$

By using boundary conditions (12) and (13) for $\mathrm{k} = 1,2$ we have:

$${P_0}^{(k)}\left({\theta_1}^k, \widetilde{\xi_j^k},\right) = 0, \quad j = 1,2,\ldots,M-1, k = 1,2 \qquad (26)$$

$$P_0^{(k)}\left(\theta_2^{k}, \widetilde{\xi_J^{k}}, \right) = 0, \quad j = 1,2,\dots,M-1, k = 1,2 \quad (27)$$

$$P_0^{(1)}\left(\widetilde{\theta_i^{1}}, -\lambda\right) = 0, \; i = 0,1,\dots,\frac{N}{2}, \quad (28)$$

$$P_0^{(1)}\left(\widetilde{\theta_i^{1}}, \lambda\right) = 0, \qquad i = 0,1,\dots,\frac{N}{2}, \quad (29)$$

$$P_0^{(2)}\left(\widetilde{\theta_i^{2}}, -\lambda\right) = 0, \qquad i = \frac{N}{2}, \frac{N}{2}+1, \dots, N, \quad (30)$$

$$\mathrm{P_0}^{(2)}\left(\widetilde{\theta_1^{2}}, -\lambda\right) = 0, \qquad \mathrm{i} = \frac{\mathrm{N}}{2}, \frac{\mathrm{N}}{2}+1, \dots, \mathrm{N} \quad (31)$$

From Fig. 3 it can be concluded that

$$\mathrm{P_0}^{(1)}\left(\theta_1^{2}, \widetilde{\xi_\mathrm{J}^{1}}, \right) = \mathrm{P_0}^{(2)}\left(\theta_2^{1}, \widetilde{\xi_\mathrm{J}^{2}}, \right) = 0, \quad (32)$$

This condition guarantees the continuity of the function $\mathrm{P_0}(\theta, \xi)$ at the point $\theta = \theta_2^{1} = \theta_1^{2} = \pi$.

Two more equations are needed to be able to obtain x and y directly. We use equations (21) and (22). From these equations, and considering equation (5), since our problem is for the two lobe system, we have the following results:

$$F_x + \int_{-\lambda}^{\lambda}\int_{\theta_1^{1}}^{\theta_1^{2}} P_0^{(1)}(\theta,\xi)\cos(\theta,\xi)d\theta d\xi + \int_{-\lambda}^{\lambda}\int_{\theta_1^{2}}^{\theta_2^{2}} P_0^{(2)}(\theta,\xi)\cos(\theta,\xi)d\theta d\xi = 0, \quad (33)$$

and

$$F_y + \int_{-\lambda}^{\lambda}\int_{\theta_1^{1}}^{\theta_1^{2}} P_0^{(1)}(\theta,\xi)\sin(\theta,\xi)d\theta d\xi + \int_{-\lambda}^{\lambda}\int_{\theta_1^{2}}^{\theta_2^{2}} P_0^{(2)}(\theta,\xi)\sin(\theta,\xi)d\theta d\xi = 0, \quad (34)$$

These result in a system of $2\left(\frac{\mathrm{N}}{2}+1\right)(\mathrm{M}+1)+2$ nonlinear equations and $2\left(\frac{\mathrm{N}}{2}+1\right)(\mathrm{M}+1)+2$ unknowns, which may be solved by standard numerical methods such as the Newton's method.

## 5. Results and discussion

The results obtained by RBF collocation method presented in this paper were applied to two, three and four lobe gas journal bearings. By considering aspect ratio is unity and preload equal to 0.5, the distribution of pressure in two, three and four lobe gas bearings is shown in Figs. 4-6, respectively. The equilibrium point and power loss have been obtained by these pressures and compared with the other works. These results are shown in Table 3 for GA-RBF and IMQ-RBF. These results are in consonance with the previous results and confirm the validity of our method.

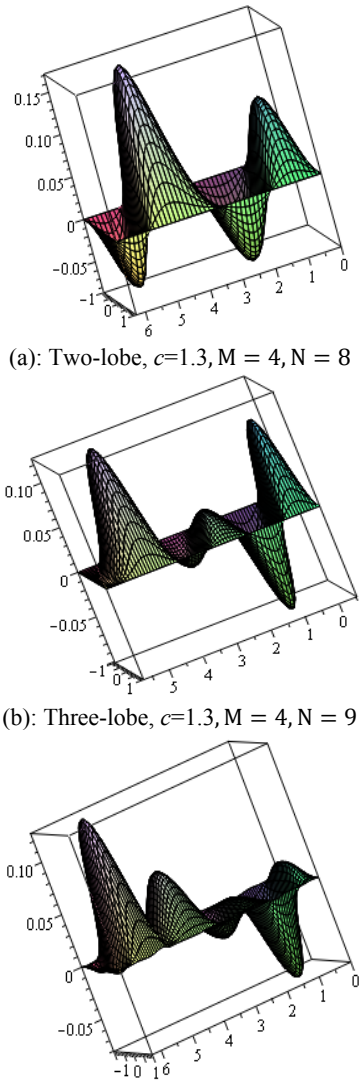

(a): Two-lobe, $c$=1.3, $\mathrm{M} = 4, \mathrm{N} = 8$

(b): Three-lobe, $c$=1.3, $\mathrm{M} = 4, \mathrm{N} = 9$

(c): Four- lobe, $c$=0.9, $\mathrm{M} = 4, \mathrm{N} = 12$

**Fig. 4.** The distribution of pressures in different lobes with $\Lambda = 2, \mathrm{F_0} = 0.2$ and $\mathrm{GA-RBF}$

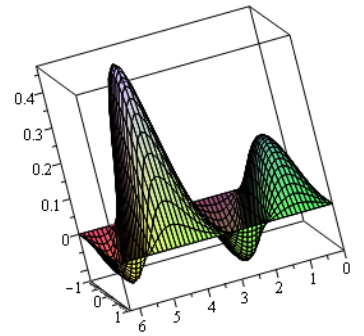

(a) Two-lobe, $c$=1.3, $\mathrm{M} = 4, \mathrm{N} = 8$

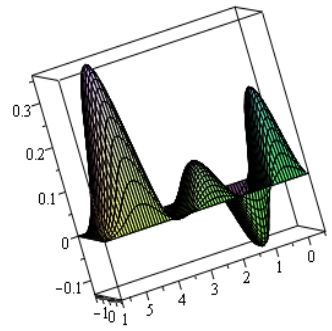

(b) Three-lobe, $c$=1.2, M = 3, N = 9

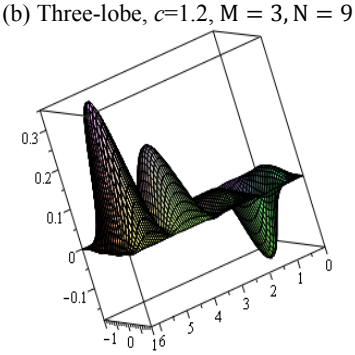

(c) Four-lobe, $c$=0.8, M = 4, N = 16

**Fig. 5.** The distribution of pressures in different lobes with $\Lambda = 5, F_0 = 0.5$ and GA − RBF

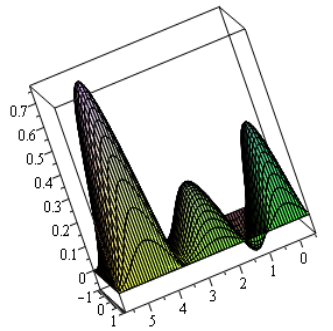

(b) Three-lobe, $c$=0.7, M = 4, N = 9

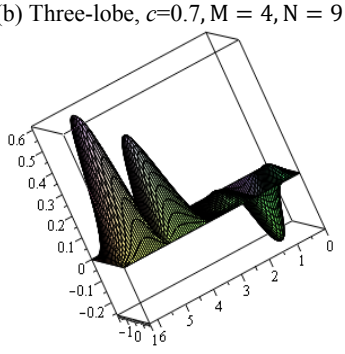

(c) Four-lobe, $c$=2.2, M = 4, N = 12

**Fig. 6.** The distribution of pressures in different lobes with $\Lambda = 10, F_0 = 1$ and GA − RBF

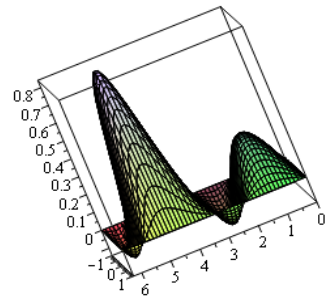

(a) Two-lobe, $c$=1.2, M = 4, N = 10

**Table 3.** Comparison of the effects of different bearing numbers and load capacity on the coordinates and pressure of gas bearings with different lobes

| Λ | $F_0$ | Bearing type | $x_j$[16] | $x_j$[25] | $x_j$-GA | $x_j$-IMQ | $y_j$[16] | $y_j$[25] | $y_j$-GA | $y_j$-IMQ | $P_L$[16] | $P_L$[25] | $P_L$-GA | $P_L$-IMQ |
|---|---|---|---|---|---|---|---|---|---|---|---|---|---|---|
| 2 | 0.2 | Two-lobe | 0.217 | 0.224 | 0.224 | 0.232 | -0.050 | -0.053 | -0.054 | -0.052 | 10.22 | 10.29 | 10.27 | 10.27 |
| | | Three-lobe | 0.209 | 0.194 | 0.222 | 0.194 | -0.071 | -0.082 | -0.089 | -0.089 | 11.26 | 11.34 | 11.40 | 11.37 |
| | | Four-lobe | 0.231 | 0.23 | 0.237 | 0.232 | -0.081 | -0.085 | -0.092 | -0.093 | 11.96 | 12.00 | 12.00 | 12.00 |
| 5 | 0.5 | Two-lobe | 0.160 | 0.166 | 0.176 | 0.169 | -0.103 | -0.111 | -0.119 | -0.114 | 10.11 | 10.16 | 10.16 | 10.17 |
| | | Three-lobe | 0.192 | 0.194 | 0.186 | 0.194 | -0.146 | -0.147 | -0.158 | -0.152 | 11.22 | 11.29 | 11.34 | 11.34 |
| | | Four-lobe | 0.227 | 0.231 | 0.286 | 0.227 | -0.154 | -0.159 | -0.196 | -0.181 | 12.01 | 12.04 | 12.28 | 12.08 |
| 10 | 1 | Two-lobe | 0.126 | 0.122 | 0.118 | 0.123 | -0.178 | -0.174 | -0.203 | -0.195 | 10.03 | 10.07 | 10.11 | 10.10 |
| | | Three-lobe | 0.126 | 0.122 | 0.124 | 0.122 | -0.178 | -0.174 | -0.198 | -0.198 | 11.29 | 11.31 | 11.27 | 11.27 |
| | | Four-lobe | 0.268 | 0.277 | 0.270 | 0.268 | -0.241 | -0.243 | -0.297 | -0.295 | 12.3 | 12.26 | 12.50 | 12.49 |

## 6. Error Analysis

Madych have proven exponential convergence property of multiquadratic approximation (Chen et al., 2003). He has shown that under certain conditions, the interpolation error is $\varepsilon = O(\lambda^{\frac{c}{h}})$ where c is the shape parameter, h is the mesh size and $0 < \lambda < 1$ is a constant. It implies the approximated solution can be improved either by reducing the size of h or by increasing the magnitude of $c$. It means that if $c \to \infty$ then $\varepsilon \to 0$. Since increasing of $c$ can improve the accuracy exponentially without extra computation (Hung et al., 2007; Chen et al., 2003; Madych, 1992), it is preferred to decrease error rather than reduce $h$.

However, according to 'uncertainty principle' of Schaback (Schaback, 1995), as the error becomes smaller, the matrix becomes more ill-conditioned; hence the solution will break down as c becomes too large. The experimental results confirm such behavior of the error values as c becomes larger. The numerical results for two lobe gas journal bearings are demonstrated in Figs. 7 and 8 which show, according to the findings of Madych, the error functions decrease exponentially as $c$ becomes larger in bounded interval. After that according to the research of Schaback the error values decline as $c$ becomes too large. The best $c$ is different for various problems and is not the same RBFs.

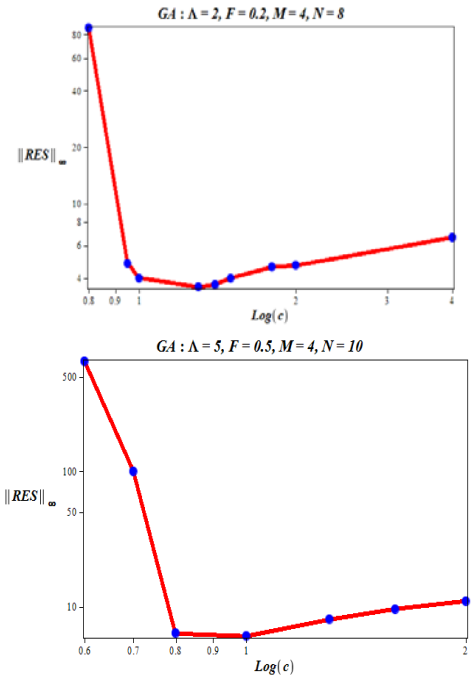


**Fig. 7**. Horizontal axis is related to shape parameter ($c$) with log mode and vertical axis shows residual error (RES) values with log mode when the solutions are approximated by using GA-RBF

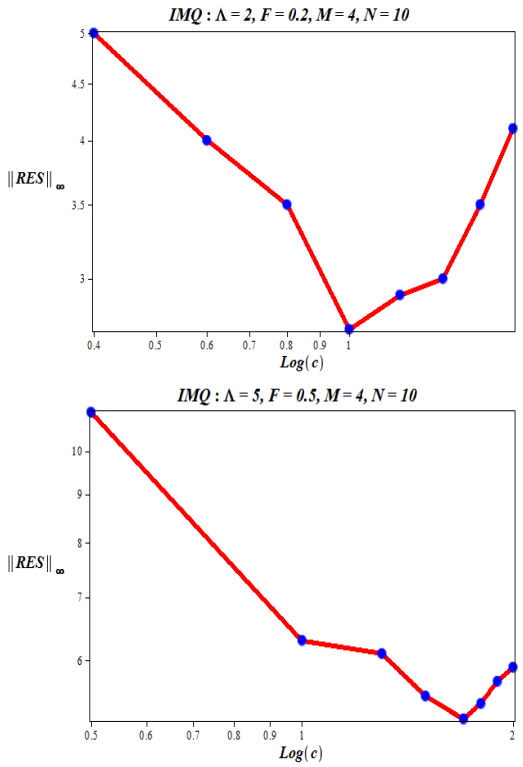


**Fig. 8**. Horizontal axis is related to shape parameter ($c$) with log mode and vertical axis shows residual error (RES) values with log mode when the solutions are approximated by using IMQ-RBF

## 7. Conclusion

In this work, based on the Radial Basis Function solutions of gas lubrication equations, the static characteristics such as the bearing load capacity, the position of rotor center and the viscous power loss is studied for three types of gas-lubricated noncircular journal bearings. The merit of our method for case study is that the equilibrium position of the rotor is obtained without using the trial and error method.

## Nomenclature

| | |
|---|---|
| c | Shape parameter |
| $\overline{C}$ | Conventional radial clearance, ( $m$ ) |
| $\overline{C}_m$ | Minor clearance when rotor and bearing geometric centers are coincident, ( $m$ ) |
| $\overline{R}$ | Rotor radius, ( $m$ ) |
| $F_{X_0}, F_{Y_0}$ | Components of the fluid film force on the rotor in the steady state, |
| $F_0$ | Load capacity |
| $h_0$ | Film thickness, |
| $L$ | Number of lobe |

| | |
|---|---|
| $\overline{L}$ | Length of bearings |
| M | The number of data points on axis θ |
| N | The number of data points on axis ξ |
| $P_0$ | Gas pressure |
| $P_0(\theta,\xi)$ | Approximate Solution of pressure |
| $\overline{P}_a$ | Ambient pressure, ( $\frac{N}{m^2}$ ) |
| $X_{j0}, Y_{j0}$ | Coordinates of the rotor center in steady state |
| $\alpha_{i,j}$ | Unknown Coefficients |
| $\delta$ | Preload in the bearing, ( $\frac{\overline{C}_m}{\overline{C}}$ ) |
| $\lambda$ | Bearing aspect ratio, ( $\frac{\overline{L}}{2\overline{R}}$ ) |
| $\Lambda$ | Bearing number |
| $\overline{\mu}$ | Ambient dynamic viscosity of the lubricant, ( $\frac{N.s}{m^2}$ ) |
| $\theta$ | Angular coordinate measured from X – axis |
| $\theta_0^k$ | Angle of lobe line of centers |
| $\theta_1^k, \theta_2^k$ | Angles at the leading and trailing edge of the lobe |
| $\overline{\omega}$ | Rotational speed of the rotor, ( $\frac{rad}{s}$ ) |
| $\xi$ | Coordinate along bearing axis measured from mid span |
| $\phi_0$ | Attitude angle |
| superscrib | |
| $k$ | Lobe designation |

## References


Baxter, B. J. C. (1992). The Interpolation Theory of Radial Basis Functions. Cambridge University.

Chandra, M., Malik, M., & Sinhasan, R. (1983). Comparative Study of Four Gas-Lubricated Noncircular Journal Bearing Configurations. *Tribology International*, 16, 103–108.

Chen, H., Kong, Li., & Leng, W. (2012). Numerical solution of PDEs via integrated radial basis function networks with adaptive training algorithm. *Applied Soft Computing*, 11, 855–860.

Cheng, A. H., Golberg, M. A., Kansa, E. J., & Zammito, G. (2003). Exponential convergence and hc multiquadric collocation method for partial differential equations. *Numerical Methods for Partial Differential Equations*, 19, 571–594.

Dag, I., & Dereli, Y. (2008). Numerical solution of KdV equation using radialbasis functions. *Applied Mathematical Modelling*, 32, 535–546.

Dehghan, M., & Shokri, A. (2009). Numerical solution of the nonlinear KleinGordon equation using radial basis functions. *Journal of Computational and Applied Mathematics*, 230, 400–410.

Dehghan, M., & Shokri, A. (2009). A meshless method for numerical solution of the one-dimensional wave equation with an integral condition using radial basisfunctions. *Numerical Algorithms*, 52, 461–477.

Frene, J. Nicolas, D. Degueurce, B. Berthe, D., & Godet M. (1997). *Hydrodynamic Lubrication: Bearing and Thrust Bearing*, V. N. Costantinescu, Elsevier, Amsterdam.

Golberg, M. A. (1999). Somerecent results and proposals for the use of radial basis functions in the BEM. *Engineering Analysis with Boundary Elements*, 23, 285–296.

Gustavo, G., Vignolo, Daniel O. Barila., & Lidia, M. Quinzani, (2011). Approximate analytical solution to Reynolds equation for finite length journal bearings. *Tribology International*, 44, 1089–1099.

Huang, C. S., Lee, C. F., & Cheng, A. H. (2007). Error estimate, optimal shape factor, and high precision computation of multiquadric collocation method. *Engineering Analysis with Boundary Elements*, 31, 614–623.

Islam, S. U., Sarler, B., Vertnik, R., & Kosec, G. (2012). Radial basis function collocation method for the numerical solution of the two-dimensional transient nonlinear coupled Burgers equations. *Applied Mathematical Modelling*, 36, 1148–1160.

Jiangang ,Y., Rui, G., & Yongwei, T. (2008). Hybrid radial basis function /finite element modelling of journal bearing. *Tribology International*, 41, 1169–1175.

Kansa, E. J. (1990). Multiquadrics a scattered data approximation scheme with applications to computational fluid dynamics. *Computers & Mathematics with Applications*, 19, 127–145.

Khattak, A. J., Tirmizi, S. I. A., & Islam, S. U. (2009). Application of meshfree collocation method to a class of nonlinear partial differential equations. *Engineering Analysis with Boundary Elements*, 33, 661–667.

Klit, P., & Lund, J. W. (1986). Calculation of the dynamic coefficients of a journal bearing using a variational approach. *Journal of Tribology*, 108, 421–424.

Lund, J. W., & Thomsen, K. K. (1978). Calculation method and data for dynamic coefficients of oil-lubricated journal bearings. *American Society of Mechanical Engineers*: Topics in Fluid Film Bearings and Rotor Bearing Systems Design and Optimization, 1–28.

Madych, W. R. (1992). Bounds on multivariate polynomials and exponential error estimates for multiquadric interpolation. *Journal of Approximation Theory*, 70, 94–114.

Madych, W. R. (1992). Miscellaeous error bounds for multiq uadratic and related interpolators. *Computers & Mathematics with Applications*, 24, 121–138.

Parand, K. & Rad, J. A. (2012). Numerical solution of nonlinear Volterra–Fredholm–Hammerstein integral equations via collocation method based on radial basis functions. *Applied Mathematics and Computation*, 218, 5292–5309.

Rahmatabadi, A. D., & Rashidi, R. (2007). Investigation of preload effects on noncircular gas bearing systems performance. *Journal of Aerospace Science and Technology*, 4, 1–6.

Rashidi, R., KaramiMohammadi, A., & BakhtiariNejad, F. (2010). Preload effect on nonlinear dynamic behavior of a rigid rotor supported by noncircular gas-

lubricated journal bearing systems. *Nonlinear dynamic*, 60, 231–253.

Rashidi, R., KaramiMohammadi, A., & BakhtiariNejad, F. (2010). Effect of Bearing Number on Nonlinear Dynamic Behavior of Aerodynamic Noncircular Journal Bearing Systems. Proceedings of the Institution of Mechanical Engineers, Part J: *Journal of Engineering Tribology*, 224, 139–154.

Rashidi, R., Karami Mohammadi, A., & BakhtiariNejad, F. (2010). Rotor Mass Effect on Nonlinear Dynamic Behavior of Aerodynamic Noncircular Journal Bearing Systems. *IJST-Trans. B*, 34, 215–230.

Rashidi, R., KaramiMohammadi, A., & BakhtiariNejad, F. (2010). Bifurcation and Nonlinear Dynamic Analysis of a Rigid Rotor Supported by Two-Lobe Noncircular Gas-Lubricated. *Journal Bearing System. Nonlinear Dynamics*, 61, 783–802.

Reddi, M. M., & Chu, T. Y. (1970). Finite-element solution of the steady state Incompressible lubrication problem. *Journal of Lubrication Technology*, 92, 524–531.

Reddi, M. M. (1969). Finite-element solution of the Incompressible lubrication problem. *Journal of Tribology*, 91, 524–533.

Schaback, R. (1995). Error estimate and condition numbers for radial basis function interpolation. Advances in Computational Mathematics, 3, 251–264.

Wang, C. C., Yau, H. T., Jang, M. J., & Yeh, Y.L. (2007). Theoretical analysis of the non-linear behavior of a flexible rotor supported by herringbone gas journal bearing. *Tribology International*, 40, 533–541.

Wang, C. C. (2007). Bifurcation analysis of an aerodynamic journal bearing system considering the effect of stationary herringbone grooves. *Choas Solitons Fractal*, 33, 1532–1545.

Zerroukat, M., Power, H., & Chen, C. S. (1998). A numerical method for heat transfer problem using collocation and radial basis functions. *International Journal for Numerical Methods in Engineering*, 42, 1263–1278.

Laca, M., & Raeburn, I. (1996). Semigroup crossed products and Toeplitz algebras of nonabelian groups. *Journal of functional analysis*, 139(2), 415–440.

Laca, M., & Raeburn, I. (1999). A semigroup crossed product arising in number theory. *Journal of the London Mathematics Society*, 59(1), 330–344.

Larsen, N. S. (2000). Non-unital semigroup crossed products. *Mathematical Proceedings of the Royal Irish Academy*, 100(2), 205–218.

Rajarama Bhat, B. V., Elliott, G. A., & Fillmore, P. A. (2000). *Lectures on operator theory, Fields Inst.* American Mathematics Society, Providence, Rhode Island.

Rieffel, M. A. (1974). Induced representations of $C^*$ −algebras. *Advances in Mathematics*, 13(2), 176–257.

Sieben, N. (1997). $C^*$ −Crossed products by partial actions and actions of inverse semigroups. *Journal of the Australian Mathematical Society*, 63(1), 32–46.

Tabatabaie Shourijeh, B. (2006). Partial Inverse Semigroup C*-algebra. *Taiwanese Journal of Mathematics*, 10(6), 1539–1548.